ISSN 0915 633X

NIFS--250

JP9404267

# Innovative Energy Production in Fusion Reactors

A. Iiyoshi, H. Momota, O. Motojima, M. Okamoto, S. Sudo,
Y. Tomita, S. Yamaguchi, M. Ohnishi, M. Onozuka, C. Uenosono

(Received – Oct. 8, 1993)

NIFS-250 Oct. 1993

# INNOVATIVE ENERGY PRODUCTION IN FUSION REACTORS

A. Iiyoshi, H. Momota, O. Motojima, M. Okamoto, S. Sudo, Y. Tomita, S. Yamaguchi, M. Ohnishi*, M. Onozuka**, C. Uenosono***

National Institute for Fusion Science, Nagoya 464-01, Japan
*Kyoto University, Uji 611, Japan
**Mitsubishi Heavy Industries, Ltd., Minato-ku, Tokyo 105, Japan
***The Kansai Electric Power Co., Inc., Kita-ku, Osaka 530, Japan

[The essential part of this paper was presented at ICENES'93, Makuhari, Japan, 1993, O-6.]

KEYWORDS: fusion reactors, neutron-lean fusion reactor, direct energy conversion, plant efficiency

# INNOVATIVE ENERGY PRODUCTION IN FUSION REACTORS

A. Iiyoshi, H. Momota, O. Motojima, M. Okamoto, S. Sudo, Y. Tomita, S. Yamaguchi, M. Ohnishi*, M. Onozuka**, C. Uenosono***

National Institute for Fusion Science, Nagoya 464-01, Japan
*Kyoto University, Uji 611, Japan
**Mitsubishi Heavy Industries, Ltd., Minato-ku, Tokyo 105, Japan
***The Kansai Electric Power Co., Inc., Kita-ku, Osaka 530, Japan

## ABSTRACT

Concepts of innovative energy production in neutron-lean fusion reactors without having the conventional turbine-type generator are proposed for improving the plant efficiency. These concepts are (a) traveling wave direct energy conversion of 14.7 MeV protons, (b) cusp type direct energy conversion of charged particles, (c) efficient use of radiation with semiconductor and supplying clean fuel in a form of hydrogen gas, and (d) direct energy conversion from deposited heat to electric power with semiconductor utilizing Nernst effect. The candidates of reactors such as a toroidal system and an open system are also studied for application of the new concepts. The study shows the above concepts for a commercial reactor are promising.

KEYWORDS: fusion reactors, neutron-lean fusion reactor, direct energy conversion, plant efficiency,

## I. INTRODUCTION

In this article, we propose innovative concepts of fusion reactor system. Part of the original motivation to start fusion research was to develop a clean energy system with abundant fuel in the earth. As research advanced, however, choices in the categories: (1) fuel, (2) confinement scheme, (3) energy conversion method have become rather limited. At present, resources and man power in the world are put mainly on the field of a D-T tokamak fusion reactor, of which representative is ITER (International Thermonuclear Experimental Reactor). It is expected that the ignition will be demonstrated with the tokamak reactor in the beginning of 21st century. On the other hand, however, it is widely recognized that the D-T tokamak reactor has the following severe problems in the reactor technology: (a) steady state operation, (b) plasma disruption, (c) large inventory of tritium and breeding, (d) radioactivation and damage of structural material by high energy neutrons.

Therefore, if we limit the fusion rector concepts in the very narrow field at this stage, it would unfavorably delay the realization of a commercial fusion reactor.

Here, we will not limit fuel species only as D-T, but study more clean advanced fuel such as catalyzed D-D [1,2] (Cat.D-D) and D-$^3$He [3,4]. Furthermore, as for concept of fusion reactor, we treat open system and FRC as well as toroidal system. Moreover, we study energy conversion methods in the wide variety of the fields such as innovative schemes of direct energy conversion from the fusion energy to electricity and to fuel hydrogen gas without having a turbine generator.

Fortunately, reliability of plasma productions and their confinements have been improved appreciably in tokamak experiments and plasma temperatures are ready to

several tens of keV which is closed to an ignition temperature of advanced fuels such as Cat.D-D or D- $^3$He.

For D-T fusion fuels, reaction:

$$D + T \rightarrow {}^4He\ (3.52MeV) + n\ (14.06MeV) \quad (1)$$

is available. The D-D reactions are negligible if the operating plasma temperature is around a ten keV. The fusion ignition is easiest with this fusion fuels. There are practically no natural resource of tritium, therefore, one has to produce it in a breeding blanket. The primary nuclear reactions of Cat.D-D fusion are:

$$D + D \rightarrow {}^3He\ (0.82MeV) + n\ (2.45MeV) \quad (2)$$

and

$$D + D \rightarrow T\ (1.01MeV) + p\ (3.03MeV). \quad (3)$$

The branching ratio of these reactions are approximately the same. One reinjects the fusion products $^3$He and T into a Cat.D-D burning plasma to produce energy through nuclear reactions with fuel deuterium. Therefore, reaction (1) may supplement the reactions (2) and (3) as well as the reaction:

$$D + {}^3He \rightarrow {}^4He\ (3.67MeV) + p\ (14.67MeV). \quad (4)$$

The primary fuel of Cat.D-D fusion is only deuterium that is naturally abundant in water and no breeding blanket is necessary. Consequently, engineering problems attributed to the tritium breeding are dissolved. The D- $^3$He fusion utilizes the reaction (4), as the primary fusion reaction. D-D reactions (2) and (3) and the D-T reaction (1) follow to this reaction.

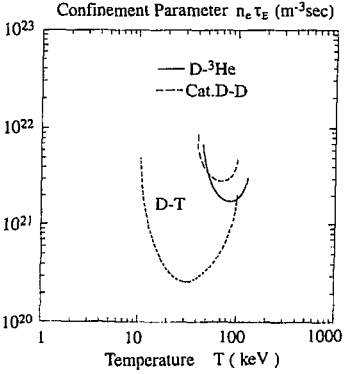


**Fig. 1 *Ignition conditions for* D-T, catalyzed D-D and D- $^3$He concepts.**

Nevertheless, the concentration of $^3He$ is large and the operation temperature is so high that effects of those accompanied reactions reduce appreciably. The natural resource of $^3He$ is, however, very poor on the Earth. One needs to develop extraterrestrial $^3He$ resources such as the Lunar surface to construct commercial D-$^3He$ fusion reactors.

The ignition conditions for Cat.D-D and D-$^3H_e$ concepts are shown in Fig. 1. The fusion powers are carried in the following three forms: (a) neutrons ($P_n$), (b) charged particles ($P_{ch}$), and (c) radiation ($P_r$).

In the fusion reactor scheme with D-T fuel cycle, 80 % of the D-T fusion energy is in 14 MeV neutrons, while 30 % of the fusion energy for Cat.D-D is in neutrons. In case of D-$^3H_e$, only a few % is in neutrons. The fraction of neutron power in fusion power with parameter of temperature is shown in Fig. 2.

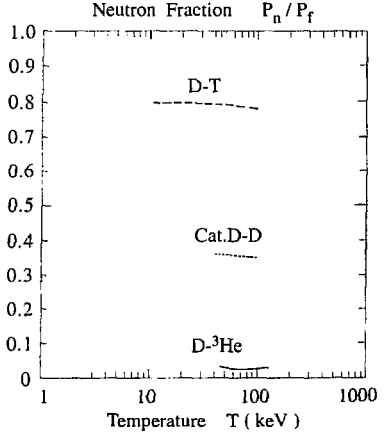


Fig. 2 Fraction of neutron power in fusion power.

## II. ADVANCED REACTOR CONCEPTS

The ignition conditions for Cat.D-D and D-$^3H_e$ reactors are shown in Fig. 3, where all charged particles stemming from fusion are assumed to be trapped in the plasma confining region, and the reflectivity of the wall surface is assumed as 0.99 (SUS material at 570 K). The bulk plasma particles (as fuel), however, have an finite confinement time as parameter. The mixing ratio of D particles to $^3H_e$ particles is taken as 1 for D-$^3H_e$.

The ratio $\eta_{ash} \equiv \tau_{ash} / \tau_E$ of ash particle confinement time $\tau_{ash}$ to energy confinement time $\tau_E$ is assumed to be 2. This is an important factor, although it is often neglected (implicitly taken as $\eta_{ash}=0$). If $\eta_{ash}$ is unreasonably to be taken as 0,

the limit of β value decreases to 15 % for the Cat.D-D reactor. When $\eta_{ash}$ is 2, the high β value of at least 62 % is necessary.

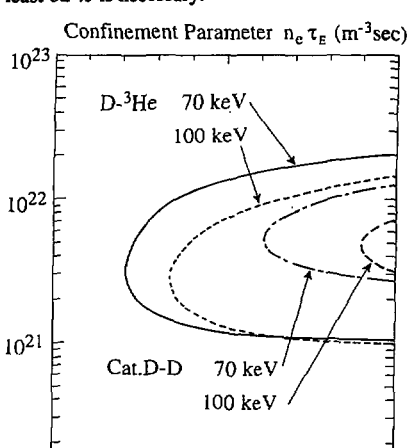


Fig. 3 Ignition condition for catalyzed D-D and D-$^3$He reactors at $\eta_{ash} \equiv \tau_{ash}/\tau_E$ =2 as a function of β value.

For a D-$^3$He reactor, the allowed lowest β value is 22 % for $\eta_{ash}$ of 2, and necessary $n_e\tau_E$ value of $8.1\times10^{20}$ sec/m$^3$ is also by a factor of several smaller than in case of Cat.D-D. Thus, the Cat.D-D is favorable in viewpoint of abundant available resources, while D-$^3$He has advantage in operation condition. Under the above condition, the dependence of fraction ratios of $P_{br}$, $P_{sy}$ and $P_{ch}$ to fusion power $P_f$ on β value may be interested for determining which scheme should be utilized mainly in a reactor. The symbols of $P_{br}$, $P_{sy}$ and $P_{ch}$ stand for bremsstrahlung radiation power, synchrotron radiation power, and the loss power of plasma fuel particles through convection and thermal conduction, respectively. The neutron power fraction for D-$^3$He is only 2-4 % which includes both contribution from D-D and D-T reactions. The latter contributes more by a factor of 1.5 - 4 than the case of the former. The neutron power fraction for Cat.D-D concept is 35 %, of which main contribution is due to D-T reaction (29 %).

For one example, the calculated power fractions are shown in Fig. 4 for D-$^3$He at $T_e$ = 70 keV and $\eta_{ash}$ = 2. As seen in the figure, the synchrotron radiation is

negligibly small except for the relatively low β value region (≤ 50 %). It should be noted that the fraction of bremsstrahlung power remains almost constant at about 30 %.

From the above results, the D-$^3He$ scheme for fuel seems most plausible. One of the appropriate devices confining the high β D-$^3He$ plasma is FRC, of which schematic drawing is shown in Fig. 5. In this case, the main power outputs are $P_p$ by 14. 7 MeV protons, $P_{br}$ and $P_{ch}$. $P_n$ by neutrons and $P_{sy}$ are relatively small. In an open system like FRC, the charged particles ($P_p$ and $P_{ch}$) flowing out along the magnetic field lines into open space are converted directly to electricity by the direct energy conversion system, and the radiation ($P_{br}$) is converted to electricity and/or to hydrogen gas for energy resource as will be described in the next chapter.

If we can increase the reflectivity of the wall surface, the ignition condition becomes possible under lower β values as shown in Fig. 6. This is because synchrotron radiation power can be absorbed in the plasma after multi-reflection. One of candidates for such wall material having high reflectivity is beryllium. Then, a toroidal system such as a helical system having divertor configuration with β value of ≤10 % has also a chance to a commercial reactor [5]. In such a low β D-$^3He$ toroidal device, the synchrotron radiation ($P_{sy}$) becomes large (order of 50 %).

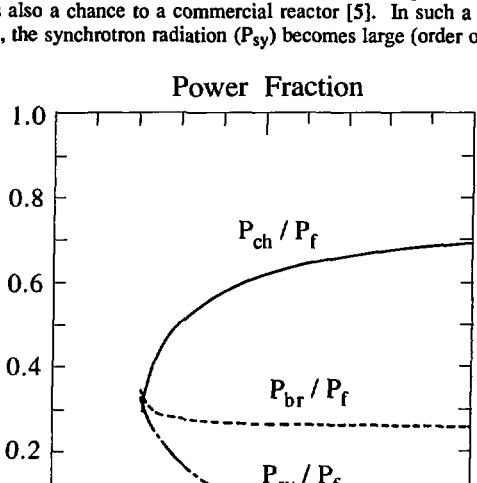


Fig. 4 Calculated power fraction for D-$^3He$ at $T_e$ = 70 keV and $\eta_{ash} \equiv \tau_{ash} / \tau_E$ =2.

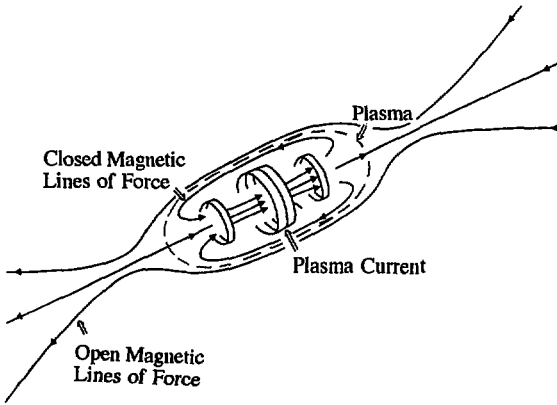


Fig. 5 Schematic drawing of FRC.

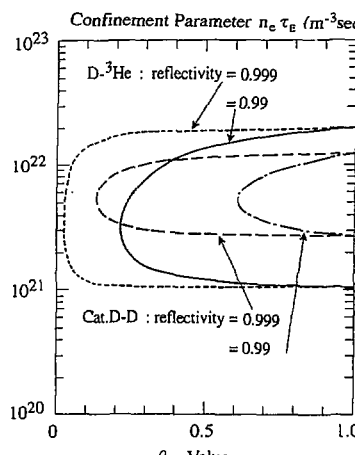


Fig. 6 Ignition condition with parameter of wall reflectivity.

A method of direct energy conversion from the synchrotron radiation to electricity using "rectena" (solid-state rectifying antenna receiving high frequency wave beginning at over 2500 GHz) was proposed by Kulcinski et al. in case of APOLLO D - $^3$He tokamak fusion reactor [3]. In contrast to this, we propose a new

concept. The synchrotron radiation as well as neutrons are once changed to thermal energy, and then, the direct energy conversion is carried out from thermal energy to electricity by using the Nernst effect, as will be described in the next chapter.

## III. CONCEPTS OF DIRECT ENERGY CONVERSION

*A. Direct Energy Conversion (DEC) of Particle Energy*

A typical example of direct energy conversion has been presented in a D-$^3$He fueled fusion reactor design ARTEMIS-L [4]. The geometry of the reactor is linear and a pair of direct energy converter systems are installed at both end of the reactor. A converter system has a cusp type direct energy converter (Cusp DEC) and a traveling wave direct energy converter (TW DEC). The schematic view of Cusp DEC and TWDEC is shown in Fig.7.

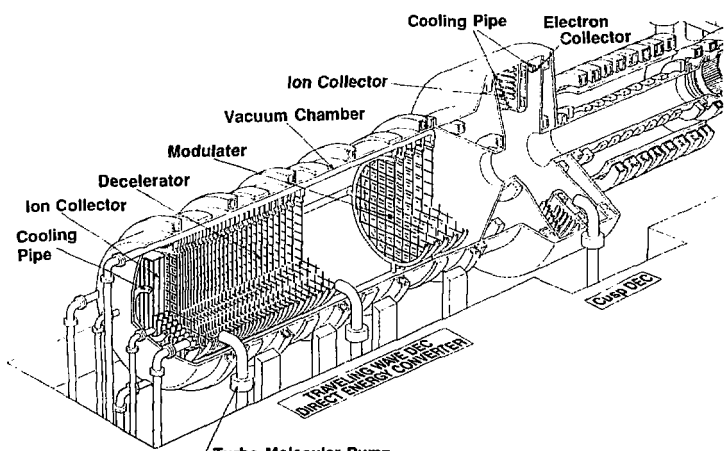


Fig. 7 Schematic view of Cusp DEC and TWDEC.

The former is a double cusped shape for controlling the energy carried by leaked fuels and ashes components. The first cusp is the electron separator that separates electrons from other ion species and introduces them to collector plates installed at the first line cusp. Because of its large moment of inertia, an ion pass through the first cusp and goes to the second line cusp. Due to the applied electrostatic field, the leaked fuel ion decreases its kinetic energy and then goes to an ion collector plate. An efficiency of 65 % is estimated [6] with this cusp type direct energy converter.

TW DEC has a modulator and a decelerator. The energy of 14.7 MeV carried by fusion protons is too high to handle with an electrostatic device. TWDEC controls this high energy particle on the base of the principle of a Linac. Because of their high energy, fusion protons pass through Cusp DEC. Then, an applied traveling electric wave moderates the velocity of the proton beam at the modulator and the proton beam forms a bunch at the entrance of the decelerator at downstream. The decelerator has a set of meshed grids, each of which are connected to a transmission circuit. One has to adjust the location of bunched protons in a decelerate phase of the traveling wave. The phase velocity of the transmission circuit also decreases as in case of protons. Protons, therefore, decrease their velocity along the stream. The kinetic energy of 14.7 MeV protons changes to an oscillating electromagnetic energy in the transmission circuit with an efficiency of 76 % [7].

*B. Direct Electron-Hole Pair Production With Radiation*

The well known device to utilize the radiation energy from the sun is a solar battery, which is typically made of p-n junction of silicon semiconductor. If the light having energy more than the band gap energy is illuminated on the semiconductor, electron-hole pairs are produced in the region of the p-n junction. This can cause current, and thus, electric power. Unfortunately, due to the low equivalent temperature spectrum of the sun light, the available photons are limited. In contrast to this, the spectrum of the radiation from the fusion plasma has a much higher equivalent temperature. Then, the available photons to produce electron-hole pairs are abundant. So, the radiation from the fusion plasma may efficiently induce current in the semiconductor.

On the other hand, Fujishima and Honda found that an only p-type or n-type semiconductor such as $TiO_2$ illuminated by photons having more than certain energy can be used for electrolysis of water [8]. The process has been well explained with energy band configuration of a semiconductor immersed in the liquid electrolyte. For example, the process for $TiO_2$ can be considered as follows:

$$TiO_2 + h\nu \rightarrow e^- + p^+$$
$$H_2O + 2p^+ \rightarrow 1/2O_2 + 2H^+ \quad \text{(at } TiO_2 \text{ electrode)}$$
$$2H^+ + 2e^- \rightarrow H_2 \quad \text{(at Pt electrode)}$$

The energy level of the conduction (and also valence) band increases near the surface of semiconductor $TiO_2$ facing the liquid electrolyte. If the photon having energy larger than the band gap energy $\varepsilon_g$ of the semiconductor ($\varepsilon_g$= 3 eV in case of $TiO_2$) is illuminated on the semiconductor, electron-hole pair(s) are produced, and the electron excited into the conduction band moves the opposite direction to the surface of semiconductor facing the liquid electrolyte, while the hole in the valence band moves to the surface of the semiconductor facing the liquid electrolyte. Thus, if the semiconductor is connected to the other electrode also immersed in the liquid electrolyte with a conducting wire, electrolysis of water can occur: oxygen gas appears at the $TiO_2$ electrode, and hydrogen gas appears at the other electrode. The principle of direct hydrogen production [9] is shown in Fig. 8, where the membrane to separate hydrogen and oxygen gases is not shown for simplicity.

For estimating conversion efficiency, "radiation ionization energy" $\varepsilon_i$ (eV) defined as the average energy required to form one electron-hole pair in semiconductor materials is a useful concept:

$$\varepsilon_i = c_0 \varepsilon_g + c_1$$

where $c_0$ and $c_1$ are constants, experimentally obtained as 14/5 and 0.5 - 1.0 (eV), respectively [10]. These two constants are fortunately independent from the form of energy source, that is, applicable all to alpha particles, electrons, and photons.

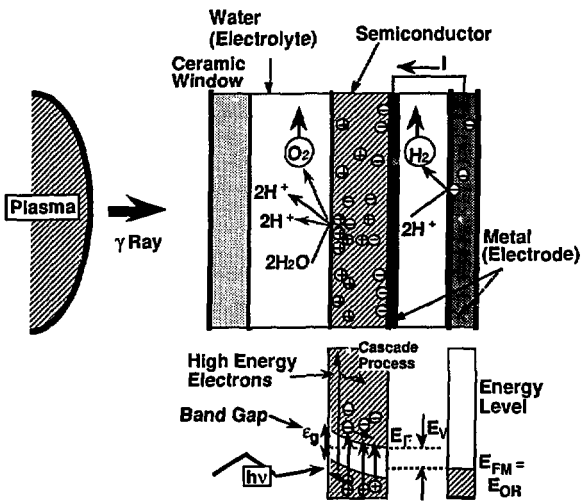


Fig. 8 Principle of direct hydrogen production by γ rays.

The efficiency $\eta_{sem}$ of direct current production by photons in the semiconductor is given as:

$$\eta_{sem} = \eta_s \eta_w \eta_m (E_V / \varepsilon_g) / (c_0 + c_1 / \varepsilon_g)$$

where $\eta_s$, $\eta_w$, $\eta_m$ are ratio of available surface area to the vacuum chamber wall, transparency of photons through the first wall, and efficiency of deposition of photon energy on the semiconductors, respectively, and, $E_V = E_F - E_{OR}$, where $E_F$ and $E_{OR}$ are the Fermi energy level of the semiconductor, and oxidation-reduction potential of the electrode immersed in the liquid electrolyte, respectively.

The efficiency $\eta_{hyd}$ of direct hydrogen production by photons in the semiconductor is given as with Faraday constant:

$$\eta_{hyd} = \eta_s \eta_w \eta_m \Delta H_f / (2F\varepsilon_i)$$

where $\Delta H_f$ is the enthalpy change by burning hydrogen gas (285.8 kJ/mol at 298 K). The main reason for determining limit of efficiency comes from the fact that ionization energy $\varepsilon_i$ is by a factor of about 3 larger than the band gap energy $\varepsilon_g$ as described. The harmful effects on semiconductors by neutrons are usually concerned. In this article, however, we consider the case that the neutron dose is rather low. We estimate the effect is negligible. Furthermore, there may be a possibility to find the adequate material of the semiconductor for this purpose.

Two cases are considered here. In Case 1, $\varepsilon_g$ and $\eta_m$ are assumed to be 3.0 eV (such as for $TiO_2$), 0.49, respectively. Then, the energy conversion ratio $\eta_{sem}$ becomes 0.10, and the hydrogen production efficiency $\eta_{hyd}$ is 0.06. In Case 2, $\varepsilon_g$ and $\eta_m$ are taken as 1.5 eV, 0.80, respectively. Then, $\eta_{sem}$ and $\eta_{hyd}$ are 0.14 and 0.18, respectively. Thus, the direct hydrogen production is favorable in Case 2. It is essential to find appropriate materiel for such a system.

The rest of radiation energy is converted to heat due to phonon excitation in the semiconductor.

*C. Thermoelectric Conversion*

Heat load from plasma through radiation and particles is directly converted to electricity with conventional thermoelectric method such as using temperature gradient and also a new method using Nernst effect (thermoelectric effect in the presence of magnetic field).[11]:

$$\mathbf{E} = \mathbf{J}/\sigma + S\nabla T + R_B \mathbf{B} \times \mathbf{J} + N\mathbf{B} \times \nabla T$$

where $\sigma$, $S$, $R_B$, and $N$ are electrical conductivity of the semiconductor, and coefficients for thermoelectric, Hall, and Nernst effects, respectively.
The schematic configuration of using the Nernst effect is shown in Fig. 9.
The conversion efficiency $\eta_t$ is given as:

$$\eta_t = \eta_{ca} / \{1 + 2\eta_{ca} / r_t + (1 + r_t)^2 / r_t Z_t T_h\}$$

where $\eta_{ca} = \Delta T / T_h$, $r_t = R_L / R_e$ , and $\Delta T$, $T_h$ , $R_L$, and $R_e$ are temperature difference, temperature of the hot side, external resistance of the circuit, and internal resistance, respectively. For conventional thermoelectric effect,

$$Z_t = \sigma C_t^2 / \kappa$$

where $C_t$, and $\kappa$ are thermoelectric coefficient and thermal conductivity of the semiconductor, respectively.

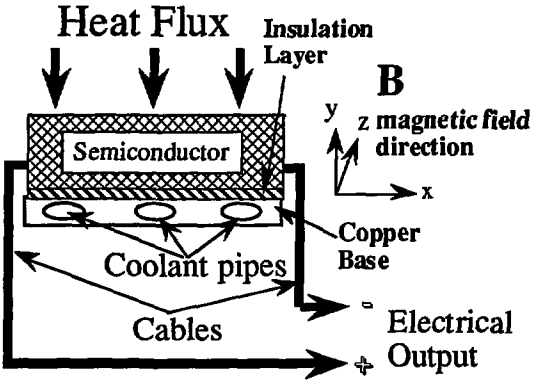


Fig. 9. Schematic configuration of the heat conversion device using the Nernst effect.

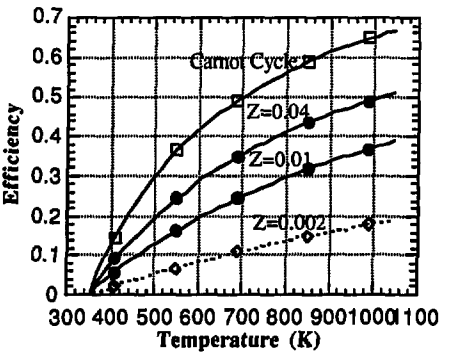


Fig. 10 Efficiency of thermoelectric and Nernst effects.

For Nernst effect,

$$Z_t = \sigma C_n^2 B^2 / \kappa$$

where $C_n$ and $B$ are Nernst coefficient and magnetic field strength, respectively.

In case of $T_h - \Delta T = 350$ K and $B = 5$ T, the relation between $\eta_t$ and $\Delta T$ is shown in Fig. 10, where the ideal Carnot cycle, conventional thermoelectric effect, and Nernst effect are shown. When $\Delta T = 300$ K, we get $\eta_t = 0.22$ ($Z_t$=0.01) with Nernst effect, while $\eta_t = 0.1$ ($Z_t$=0.002) with thermoelectric effect. The case for $B = 10$ T is also shown as $Z_t$=0.04, which improves the efficiency to $\eta_t = 0.32$. Thus, Nernst effect may play a dominant role in the direct energy conversion of heat.

This system is applicable to the toroidal reactors as well as to the open system, and it may be replaced with a conventional turbine generator for converting thermal energy to electricity, as the conversion efficiency might be rather higher under the optimum condition.

## IV. DESIGN CONSIDERATION OF SYSTEM PLANT

The new scheme of a fusion reactor system involving the above concepts seems promising as an advanced reactor of next generation such as innovative Cat.D-D or D-$^3$He fusion reactors with high temperature.

Candidates for the D-$^3$He reactor concept has been proposed for tokamak [3] and FRC (Field-Reversed Configuration, a typical design is ARTEMIS-L [11]).

In case of 1 GW electricity output for ARTEMIS-L, the power flow is shown in Fig. 11. The higher electricity output is, however, preferable for better plant efficiency. Such optimization is the one of subjects to be studied in future.

The total conversion efficiency $\eta_{tot}$ is given as:

$$\eta_{tot} = P_{out}^{total} / P_f$$

where

$$P_{out}^{total} = \eta_p P_p + \eta_c P_{ch} + \eta_{hyd} P_{br} + \eta_t \{(1-\eta_{hyd}) P_{br} + (1-\eta_c) P_{ch} + P_{sy} + P_n\}$$

$$P_f = P_p + P_{ch} + P_{br} + P_{sy} + P_n \quad .$$

Using $\eta_p = 0.76$, $\eta_c = 0.65$, $\eta_{hyd} = 0.18$, $\eta_t = 0.22$-$0.32$, we get total efficiency: $\eta_{tot} = 0.59$-$0.64$.

As indicated in Fig. 11, the indirect hydrogen gas production through the electrolysis with produced electricity from the fusion reactor can be also used for energy reservoir. If the commercial needs of electricity become low in night for example, the excessive electric power can be stored in the form of hydrogen gas. The efficiency of electrolysis of water is rather high (more than 90 %) within the

present state of art. Thus, both the direct and indirect hydrogen production scheme is attractive from the viewpoint of efficiency and flexible energy storage.

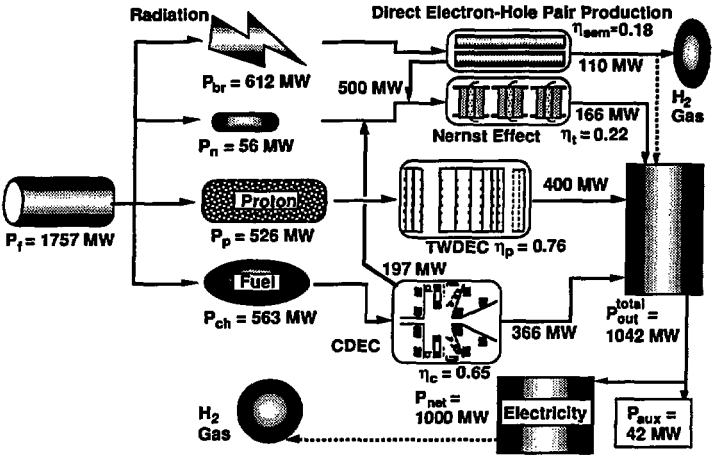


Fig. 11 Power flow for ARTEMIS-L having 1 GW electricity output.

The image of the total plant system is shown in Fig. 12, where the energy system consists of electricity and hydrogen gas.

## V. CONCLUSION

Concepts of innovative energy production in neutron-lean fusion reactors without having a conventional turbine-type generator are proposed for improving the plant efficiency. These concepts are (a) traveling wave direct energy conversion of 14. 7 MeV protons, (b) cusp type direct energy conversion of charged particles, (c) efficient use of radiation with semiconductor and supplying clean fuel in a form of hydrogen gas, and (d) direct energy conversion from deposited heat to electric power with Nernst effect. The candidates of reactors are also studied for application of the new concepts. The example of power flow is also shown.

## ACKNOWLEDGMENT

The authors acknowledge Dr. T. Kato for information about interaction between photons and materials, and Dr. M. Sasao about interaction between neutrons and materials.

## REFERENCES


[1] K. Evans, C. C. Baker, et al., Nucl. Technology / Fusion 4(1983)226.
[2] A. Iiyoshi, O. Motojima, et al., in Proc. of 7th Symp. on Engineering Problems on Fusion Research, Knoxville, U.S.A., (1977)1683.
[3] G. L. Kulcinski, G. A. Emmert, et al., Fusion Technology, 15(1989)1233.
[4] H. Momota, A. Ishida, et al., Fusion Technology, 21(1992)2307.
[5] K. Uo, A. Iiyoshi, et al., in Plasma Physics and Controlled Nuclear Fusion Research 1982 (Proc. 9th Int. Conf. Baltimore, 1982) Vol.II, IAEA, Vienna, (1983) 209.
[6] Y. Tomita, et al., Makuhari, Japan, 1993, (AP-47).
[7] H. Momota, LA-11808C (Los Alamos, U.S.A., 1990).
[8] A. Fujishima and K. Honda, Nature, 238(1972)37.
[9] S. Sudo, et al, Makuhari, Japan, 1993, (BP-26).
[10] C. A. Klein, Jour. Appl. Phys. 39(1968)2029.
[11] S. Yamaguchi, et al, ICENES'93, Makuhari, Japan, 1993, (BP-25).
[12] H. Momota, et al., Makuhari, Japan, 1993, (AP-46).

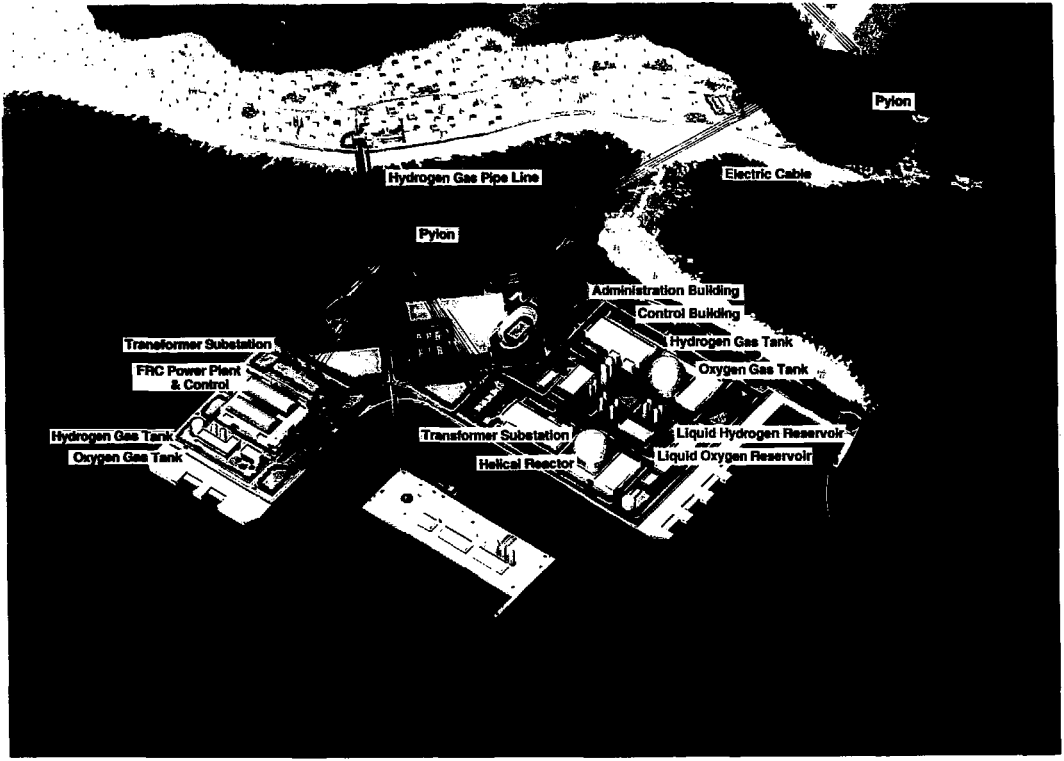


Fig. 12 Image of the total plant system "Fusion Dream Island".

## Recent Issues of NIFS Series

NIFS-197 T. Kato and K. Masai, *X-ray Spectra from Hinotori Satellite and Suprathermal Electrons* ; Oct. 1992

NIFS-198 K. Toi, S. Okamura, H. Iguchi, H. Yamada, S. Morita, S. Sakakibara, K. Ida, K. Nishimura, K. Matsuoka, R. Akiyama, H. Arimoto, M. Fujiwara, M. Hosokawa, H. Idei, O. Kaneko, S. Kubo, A. Sagara, C. Takahashi, Y. Takeiri, Y. Takita, K. Tsumori, I. Yamada and H. Zushi, *Formation of H-mode Like Transport Barrier in the CHS Heliotron / Torsatron* ; Oct. 1992

NIFS-199 M. Tanaka, *A Kinetic Simulation of Low-Frequency Electromagnetic Phenomena in Inhomogeneous Plasmas of Three-Dimensions* ; Nov. 1992

NIFS-200 K. Itoh, S.-I. Itoh, H. Sanuki and A. Fukuyama, *Roles of Electric Field on Toroidal Magnetic Confinement*, Nov. 1992

NIFS-201 G. Gnudi and T. Hatori, *Hamiltonian for the Toroidal Helical Magnetic Field Lines in the Vacuum*; Nov. 1992

NIFS-202 K. Itoh, S.-I. Itoh and A. Fukuyama, *Physics of Transport Phenomena in Magnetic Confinement Plasmas*; Dec. 1992

NIFS-203 Y. Hamada, Y. Kawasumi, H. Iguchi, A. Fujisawa, Y. Abe and M. Takahashi, *Mesh Effect in a Parallel Plate Analyzer*; Dec. 1992

NIFS-204 T. Okada and H. Tazawa, *Two-Stream Instability for a Light Ion Beam -Plasma System with External Magnetic Field;* Dec. 1992

NIFS-205 M. Osakabe, S. Itoh, Y. Gotoh, M. Sasao and J. Fujita, *A Compact Neutron Counter Telescope with Thick Radiator (Cotetra) for Fusion Experiment*; Jan. 1993

NIFS-206 T. Yabe and F. Xiao, *Tracking Sharp Interface of Two Fluids by the CIP (Cubic-Interpolated Propagation) Scheme*, Jan. 1993

NIFS-207 A. Kageyama, K. Watanabe and T. Sato, *Simulation Study of MHD Dynamo : Convection in a Rotating Spherical Shell*; Feb. 1993

NIFS-208 M. Okamoto and S. Murakami, *Plasma Heating in Toroidal Systems*; Feb. 1993

NIFS-209 K. Masai, *Density Dependence of Line Intensities and Application to Plasma Diagnostics*; Feb. 1993

NIFS-210 K. Ohkubo, M. Hosokawa, S. Kubo, M. Sato, Y. Takita and T. Kuroda,

*R&D of Transmission Lines for ECH System* ; Feb. 1993

NIFS-211 A. A. Shishkin, K. Y. Watanabe, K. Yamazaki, O. Motojima, D. L. Grekov, M. S. Smirnova and A. V. Zolotukhin, *Some Features of Particle Orbit Behavior in LHD Configurations*; Mar. 1993

NIFS-212 Y. Kondoh, Y. Hosaka and J.-L. Liang, *Demonstration for Novel Self-organization Theory by Three-Dimensional Magnetohydrodynamic Simulation*; Mar. 1993

NIFS-213 K. Itoh, H. Sanuki and S.-I. Itoh, *Thermal and Electric Oscillation Driven by Orbit Loss in Helical Systems*; Mar. 1993

NIFS-214 T. Yamagishi, *Effect of Continuous Eigenvalue Spectrum on Plasma Transport in Toroidal Systems*; Mar. 1993

NIFS-215 K. Ida, K. Itoh, S.-I.Itoh, Y. Miura, JFT-2M Group and A. Fukuyama, *Thickness of the Layer of Strong Radial Electric Field in JFT-2M H-mode Plasmas*; Apr. 1993

NIFS-216 M. Yagi, K. Itoh, S.-I. Itoh, A. Fukuyama and M. Azumi, *Analysis of Current Diffusive Ballooning Mode*; Apr. 1993

NIFS-217 J. Guasp, K. Yamazaki and O. Motojima, *Particle Orbit Analysis for LHD Helical Axis Configurations* ; Apr. 1993

NIFS-218 T. Yabe, T. Ito and M. Okazaki, *Holography Machine HORN-1 for Computer-aided Retrieve of Virtual Three-dimensional Image* ; Apr. 1993

NIFS-219 K. Itoh, S.-I. Itoh, A. Fukuyama, M. Yagi and M. Azumi, *Self-sustained Turbulence and L-Mode Confinement in Toroidal Plasmas* ; Apr. 1993

NIFS-220 T. Watari, R. Kumazawa, T. Mutoh, T. Seki, K. Nishimura and F. Shimpo, *Applications of Non-resonant RF Forces to Improvement of Tokamak Reactor Performances Part I: Application of Ponderomotive Force* ; May 1993

NIFS-221 S.-I. Itoh, K. Itoh, and A. Fukuyama, *ELMy-H mode as Limit Cycle and Transient Responses of H-modes in Tokamaks* ; May 1993

NIFS-222 H. Hojo, M. Inutake, M. Ichimura, R. Katsumata and T. Watanabe, *Interchange Stability Criteria for Anisotropic Central-Cell Plasmas in the Tandem Mirror GAMMA 10* ; May 1993

NIFS-223 K. Itoh, S.-I. Itoh, M. Yagi, A. Fukuyama and M. Azumi, *Theory of Pseudo-Classical Confinement and Transmutation to L-Mode*; May

1993

NIFS-224 M. Tanaka, *HIDENEK: An Implicit Particle Simulation of Kinetic-MHD Phenomena in Three-Dimensional Plasmas;* May 1993

NIFS-225 H. Hojo and T. Hatori, *Bounce Resonance Heating and Transport in a Magnetic Mirror;* May 1993

NIFS-226 S.-I. Itoh, K. Itoh, A. Fukuyama, M. Yagi, *Theory of Anomalous Transport in H-Mode Plasmas;* May 1993

NIFS-227 T. Yamagishi, *Anomalous Cross Field Flux in CHS ;* May 1993

NIFS-228 Y. Ohkouchi, S. Sasaki, S. Takamura, T. Kato, *Effective Emission and Ionization Rate Coefficients of Atomic Carbons in Plasmas;* June 1993

NIFS-229 K. Itoh, M. Yagi, A. Fukuyama, S.-I. Itoh and M. Azumi, *Comment on 'A Mean Field Ohm's Law for Collisionless Plasmas;* June 1993

NIFS-230 H. Idei, K. Ida, H. Sanuki, H. Yamada, H. Iguchi, S. Kubo, R. Akiyama, H. Arimoto, M. Fujiwara, M. Hosokawa, K. Matsuoka, S. Morita, K. Nishimura, K. Ohkubo, S. Okamura, S. Sakakibara, C. Takahashi, Y. Takita, K. Tsumori and I. Yamada, *Transition of Radial Electric Field by Electron Cyclotron Heating in Stellarator Plasmas;* June 1993

NIFS-231 H.J. Gardner and K. Ichiguchi, *Free-Boundary Equilibrium Studies for the Large Helical Device,* June 1993

NIFS-232 K. Itoh, S.-I. Itoh, A. Fukuyama, H. Sanuki and M. Yagi, *Confinement Improvement in H-Mode-Like Plasmas in Helical Systems,* June 1993

NIFS-233 R. Horiuchi and T. Sato, *Collisionless Driven Magnetic Reconnection,* June 1993

NIFS-234 K. Itoh, S.-I. Itoh, A. Fukuyama, M. Yagi and M. Azumi, *Prandtl Number of Toroidal Plasmas;* June 1993

NIFS-235 S. Kawata, S. Kato and S. Kiyokawa , *Screening Constants for Plasma;* June 1993

NIFS-236 A. Fujisawa and Y. Hamada, *Theoretical Study of Cylindrical Energy Analyzers for MeV Range Heavy Ion Beam Probes;* July 1993

NIFS-237 N. Ohyabu, A. Sagara, T. Ono, T. Kawamura and O. Motojima, *Carbon Sheet Pumping;* July 1993

NIFS-238 K. Watanabe, T. Sato and Y. Nakayama, *Q-profile Flattening due to Nonlinear Development of Resistive Kink Mode and Ensuing Fast Crash in Sawtooth Oscillations;* July 1993

NIFS-239 N. Ohyabu, T. Watanabe, Hantao Ji, H. Akao, T. Ono, T. Kawamura, K. Yamazaki, K. Akaishi, N. Inoue, A. Komori, Y. Kubota, N. Noda, A. Sagara, H. Suzuki, O. Motojima, M. Fujiwara, A. Iiyoshi, *LHD Helical Divertor;* July 1993

NIFS-240 Y. Miura, F. Okano, N. Suzuki, M. Mori, K. Hoshino, H. Maeda, T. Takizuka, JFT-2M Group, K. Itoh and S.-I. Itoh, *Ion Heat Pulse after Sawtooth Crash in the JFT-2M Tokamak;* Aug. 1993

NIFS-241 K. Ida, Y.Miura, T. Matsuda, K. Itoh and JFT-2M Group, *Observation of non Diffusive Term of Toroidal Momentum Transport in the JFT-2M Tokamak;* Aug. 1993

NIFS-242 O.J.W.F. Kardaun, S.-I. Itoh, K. Itoh and J.W.P.F. Kardaun, *Discriminant Analysis to Predict the Occurrence of ELMS in H-Mode Discharges;* Aug. 1993

NIFS-243 K. Itoh, S.-I. Itoh, A. Fukuyama, *Modelling of Transport Phenomena;* Sep. 1993

NIFS-244 J. Todoroki, *Averaged Resistive MHD Equations;* Sep. 1993

NIFS-245 M. Tanaka, *The Origin of Collisionless Dissipation in Magnetic Reconnection;* Sep. 1993

NIFS-246 M. Yagi, K. Itoh, S.-I. Itoh, A. Fukuyama and M. Azumi, *Current Diffusive Ballooning Mode in Seecond Stability Region of Tokamaks;* Sep. 1993

NIFS-247 T. Yamagishi, *Trapped Electron Instabilities due to Electron Temperature Gradient and Anomalous Transport;* Oct. 1993

NIFS-248 Y. Kondoh, *Attractors of Dissipative Structure in Three Disspative Fluids;* Oct. 1993

NIFS-249 S. Murakami, M. Okamoto, N. Nakajima, M. Ohnishi, H. Okada, *Monte Carlo Simuation Study of the ICRF Minority Heating in the Large Helical Device;* Oct. 1993